High-Throughput Cell-Based Screening of 4910 Known Drugs and Drug-like Small Molecules Identifies Disulfiram as an Inhibitor of Prostate Cancer Cell Growth

Kristiina Iljin,[1,2] Kirsi Ketola,[2] Paula Vainio,[2] Pasi Halonen,[1] Pekka Kohonen,[2] Vidal Fey,[1] Roland C. Grafström,[1,3] Merja Perälä,[1] and Olli Kallioniemi[1,2,4]

Abstract

Purpose: To identify novel therapeutic opportunities for patients with prostate cancer, we applied high-throughput screening to systematically explore most currently marketed drugs and drug-like molecules for their efficacy against a panel of prostate cancer cells.

Experimental Design: We carried out a high-throughput cell-based screening with proliferation as a primary end-point using a library of 4,910 drug-like small molecule compounds in four prostate cancer (VCaP, LNCaP, DU 145, and PC-3) and two nonmalignant prostate epithelial cell lines (RWPE-1 and EP156T). The EC_{50} values were determined for each cell type to identify cancer selective compounds. The *in vivo* effect of disulfiram (DSF) was studied in VCaP cell xenografts, and gene microarray and combinatorial studies with copper or zinc were done *in vitro* for mechanistic exploration.

Results: Most of the effective compounds, including antineoplastic agents, were nonselective and found to inhibit both cancer and control cells in equal amounts. In contrast, histone deacetylase inhibitor trichostatin A, thiram, DSF, and monensin were identified as selective antineoplastic agents that inhibited VCaP and LNCaP cell proliferation at nanomolar concentrations. DSF reduced tumor growth *in vivo*, induced metallothionein expression, and reduced DNA replication by downregulating MCM mRNA expression. The effect of DSF was potentiated by copper *in vitro*.

Conclusions: We identified three novel cancer-selective growth inhibitory compounds for human prostate cancer cells among marketed drugs. We then validated DSF as a potential prostate cancer therapeutic agent. These kinds of pharmacologically well-known molecules can be readily translated to *in vivo* preclinical studies and clinical trials. (Clin Cancer Res 2009;15(19):6070–8)

Downloaded from http://aacrjournals.org/clincancerres/article-pdf/15/19/6070/1983348/6070.pdf by guest on 13 June 2024

Besides surgery and radiation therapy, androgen deprivation remains the main first-line therapeutic option for prostate cancer patients, and the predominant therapy for patients with advanced and metastatic disease. However, hormonal therapy is not curative, and often, androgen-independent, drug-resistant disease develops. Such tumors remain virtually impossible to treat with current medications. The median survival time for men with androgen-independent cancer is around 2 years underlining the need to develop better therapies (1).

The majority of prostate tumors from patients with an androgen-independent disease overexpress androgen receptor (AR), thereby sensitizing prostate cancer cells to low levels of androgens. Also other mechanisms behind androgen independency have been described, such as AR mutations activating the receptor in response to nonandrogenic ligands (2). Because AR plays an essential role also in androgen-independent prostate cancers, AR and its coregulators are potential drug targets for the disease. Recently, a frequent gene fusion between the androgen-regulated prostate-specific protease TMPRSS2 and the ERG transcription factor was discovered (3). In addition to TMPRSS2-ERG, other driver genes, as well as oncogenic ETS factors (e.g., ETV1, ETV4, and ETV5) have been identified as gene fusions in prostate tumors. It has been shown that ERG fusion gene may be bypassed at later stages of cancer progression, indicating

Authors' Affiliations: [1]Medical Biotechnology, VTT Technical Research Centre of Finland, Turku; [2]Turku Centre for Biotechnology, University of Turku, Turku, Finland; [3]Institute of Environmental Medicine, Karolinska Institutet, Stockholm, Sweden; and [4]Institute for Molecular Medicine, Finland (FIMM), University of Helsinki, Helsinki, Finland

Received 4/23/09; revised 6/17/09; accepted 6/17/09; published OnlineFirst 9/29/09.

Grant support: Marie Curie Canceromics (MEXT-CT-2003-2728), EU-PRIMA project (contract # LSHC-CT-204-504587), Academy of Finland, Cancer Organizations of Finland, and Sigrid Juselius Foundation.

The costs of publication of this article were defrayed in part by the payment of page charges. This article must therefore be hereby marked *advertisement* in accordance with 18 U.S.C. Section 1734 solely to indicate this fact.

Note: Supplementary data for this article are available at Clinical Cancer Research Online (http://clincancerres.aacrjournals.org/).

Requests for reprints: Olli Kallioniemi, Institute for Molecular Medicine, University of Helsinki and Medical Biotechnology, VTT Technical Research Centre of Finland, Itäinen Pitkäkatu 4, Turku, Finland. Phone: 358-40-5698192; Fax: 358-20-722-2840. E-mail: Olli.Kallioniemi@vtt.fi.

© 2009 American Association for Cancer Research.

doi:10.1158/1078-0432.CCR-09-1035

Translational Relevance

Therapeutic options for advanced and hormone-refractory prostate cancer are limited and treatment responses often unsatisfactory. We explored here most currently marketed drugs and drug-like molecules for their efficacy against prostate cancer cells. Histone deacetylase (HDAC) inhibitor trichostatin A (TSA), thiram, disulfiram (DSF), and monensin were identified as the only agents that had antitumor efficacy at nanomolar concentrations without affecting nonmalignant control cells. Because DSF has a favorable safety profile, it was selected for further studies. Gene expression analyses indicated that DSF did not influence androgen receptor expression, but induced metallothionein genes and downregulated DNA replication. DSF also reduced VCaP prostate cancer xenograft growth *in vivo* but was not able to block it. Copper potentiated the antiproliferative effects of DSF in cultured prostate cancer cells, suggesting potential for increasing efficacy by combinatorial approaches. In summary, we have identified novel indications for known drugs that could be readily translated to *in vivo* preclinical studies and clinical trials.

that a more efficient treatment for these cancers would be of great clinical interest (4, 5).

The AR and ETS status of the available prostate cancer model cell lines are relatively well known. The VCaP cell line is an established model of *TMPRSS2-ERG* gene fusion–positive prostate cancers (3, 6). LNCaP cells overexpress ETV1 oncogene (7). Both VCaP and LNCaP cells express AR, which is lost in DU 145, and PC-3 cells (8). In VCaP cells, AR is wild-type, whereas in LNCaP cells, AR has a point mutation (T877A) enabling progestagens, estradiol, and antiandrogens to activate androgen signaling (9). The AR-T877A mutation has also been found from prostatic tissues derived from patients with a metastatic prostate cancer, indicating potential biological relevance (10).

In this study, we performed a cell-based screen with a library of 4,910 drug-like small molecule compounds, including most currently marketed drugs in the VCaP, LNCaP, PC-3, and DU 145 prostate cancer cells as well as in the RWPE-1 and EP156T nonmalignant prostate epithelial cells. Due to this selection of compounds analyzed, any interesting drugs that show efficacy would be possible to rapidly test *in vivo* in preclinical models and also in clinical trials. We focused our analysis toward identifying antiproliferative compounds that act in prostate cancer cells but lack impact on normal or transformed prostate epithelial cells. Of the several growth inhibitory compounds identified, we chose disulfiram (tetraethylthiuram disulfide; DSF) for further analysis in the VCaP cells.

Materials and Methods

Cells. The prostate carcinoma cell lines VCaP and DuCaP were received from Drs. Adrie van Bokhoven (University of Colorado Health Sciences Center, Denver, Colorado) and Kenneth Pienta (University of Michigan, Michigan) and were grown in RPMI 1640. LNCaP and LNCaP C4-2 cells were received from Dr. Marco Cecchini (University of Bern, Bern, Switzerland) and grown in T-Medium (Invitrogen). The prostate cell lines RWPE-1 (11), PC-3, and DU 145 were purchased from American Type Culture Collection (LGC Promochem AB), and the nonmalignant EP156T prostate epithelial cells were received from Dr. Varda Rotter (Weizmann Institute of Science, Rehovot, Israel) and grown in the media recommended by the distributor (12). Primary prostate epithelial cells were ordered from Lonza.

Compounds. Five compound libraries were used in high-throughput (HT) screenings (HTS). The libraries, summary of the compounds, and the final concentrations used in the screening plates were the following: Biomol (80 known kinase and phosphatase inhibitors; 10, 1, 0.1, and 0.01 μmol/L), LOPAC (1,280 existing Food and Drug Administration–approved drugs and other compounds with pharmacologically relevant structures; 1 and 0.1 μmol/L), IBIS (1,473 compounds derived from natural sources; 1 and 0.1 μmol/L), Microsource Spectrum (2,000 compounds including most of the known drugs and other bioactive compounds and natural products; 1 and 0.1 μmol/L), and an in-house library (77 experimental compounds; 10, 1, and 0.1 μmol/L).

For the validation of primary screens, DSF, thiram, and monensin were purchased from Sigma-Aldrich. DSF and thiram were dissolved in DMSO, whereas monensin was dissolved in methanol. $CuCl_2$ and $ZnCl_2$ were ordered from Sigma.

HTS assay. CellTiter-Blue cell viability assay (Promega, Inc.) was done in 384-well plates (Falcon). Before screening, cell number was titrated for each cell line separately to ensure that cell proliferation remained in a linear-exponential phase throughout the experiment. Plates containing 50 nL of compound stock solutions or DMSO as controls were diluted with 15 μL of cell culture media, and appropriate amount of cells (1,000-2,000 per well) were plated in 35 μL of media. After 72-h incubation, fluorometric CellTiter-Blue assay was done according to the manufacturer's instructions. The Envision Multilabel Plate Reader (Perkin-Elmer) was used for signal quantification.

Statistical methods applied for hit identification in HTS experiments included plate normalization using B-score (13). Compounds reducing cell viability by at least three SDs from the median of the controls were considered as putative hits. The SD of the null distribution was estimated using the statistically robust Huber's Estimator, winsorizing at 1.5 SDs. Classic multidimensional scaling of a data matrix, also known as principal coordinates analysis (14), was used to visualize the distances between the screens. The Pearson correlation distance measure was used for the screening data.

To obtain the absolute differences, the raw data were normalized using a loess method similar to the method implemented in the cellHTS2 R-package (15). The statistical outliers were down-weighted when a polynomial surface was fitted to the intensities within each assay plate using local regression. This ensured a robust fit, although some plates had a much higher hit-rate than others (16). The fit, representing a systematic background signal, was then subtracted from the raw signal values. The data were then $\log_2$-transformed and centered on the plate median. The following formula was used to calculate the absolute percentage-wise response: -100% + 2^loess_log_value%.

Determination of EC_{50} values. EC_{50} assays were done on 384-well plates with 2,000 cells per well plated in their respective growth media and left to attach overnight. A 10-fold dilution series (10 pmol/L-10 μmol/L) of selected compounds were added to the cells, and the plates were incubated for 48 h. Cell viability was determined with CellTiter-Blue assay described above. The EC_{50} data were analyzed with GraphPadPrism 4 software (GraphPad Software, Inc.).

Quantitative reverse transcriptase PCR. VCaP cells were grown into ~70% confluence before treatment with 1 μmol/L DSF for 6 and 24 h. Cells were harvested and total RNA was extracted using RNeasy (Qiagen) according to the manufacturer's protocol. Reverse transcription using 1 μg of total RNA was done with Applied Biosystem's cDNA syntesis kit. TaqMan gene expression probes and primers from the Universal Probe Library (Roche Diagnostics) were used to study ERG, AR, minichromosome maintenance complex genes (MCM2

Downloaded from http://aacrjournals.org/clincancerres/article-pdf/15/19/6070/1983348/6070.pdf by guest on 13 June 2024

and MCM5), metallothioneins (MT1A, MT1B, MT1F, MT1G, MT1X, and MT2A), and β-actin mRNA expression. Real-time quantitative PCR was done using ABI Prism 7900 (Applied Biosystems). Quantitation was carried out using the $_{\Delta\Delta}$CT method with RQ manager 1.2 software (Applied Biosystems). Average expression of the untreated control samples was considered for the calculation of the fold changes. mRNA expression of two to four replicate samples was studied.

siRNA transfection, RNA isolation, and real-time qPCR. siRNA molecules targeting metallotioneins and MCMs were transfected into VCaP and LNCaP cells by using reverse transfection with siLentFect transfection (Bio-Rad) reagent in Opti-MEM (Invitrogen). Four siRNA molecules were ordered from Qiagen (HP GenomeWide) against MCM5, MT1A, MT1B, MT1F, MT1G, MT1X, and MT2A and one validated siRNA molecule for MCM2. AllStars Negative Control and siRNA against PLK1 were used as controls in experiments. The final siRNA concentration was 13 nmol/L.

Western blot analysis. For protein extraction and Western blot analysis, cells were plated at 70% confluency and left to attach overnight. VCaP cells were treated with the indicated compounds for the indicated time. The cell extracts were separated by SDS-PAGE and transferred to a nitrocellulose membrane. Western blot analysis was done using specific antibodies against AR (1:1,000 dilution, mouse monoclonal, Labvision), cleaved poly ADP ribose polymerase (1:4,000 dilution, rabbit monoclonal, Abcam), and β-Actin (1:4,000 dilution, mouse-monoclonal, Becton Dickinson). Signal was detected with 1: 4,000 dilutions of appropriate horseradish peroxidase–conjugated secondary antibodies (all from Invitrogen Molecular Probes), followed by visualization with the enhanced chemiluminescence reagent (Amersham Biosciences).

Gene expression analysis using BeadArrays. VCaP cells were grown to ~70% confluency before treatments with 1 μmol/L DSF for 3, 6, and 24 h before harvesting. Total RNA was extracted using RNeasy (Qiagen) according to the manufacturer's protocol. Integrity of the RNA before hybridization was monitored using a Bioanalyzer 2100 (Agilent) according to manufacturer's instructions. Purified total RNA (500 ng) was amplified with the TotalPrep kit (Ambion) and the biotin-labeled cRNA was hybridized to Sentrix HumanRef-8 Expression

Downloaded from http://aacrjournals.org/clincancerres/article-pdf/15/19/6070/1983348/6070.pdf by guest on 13 June 2024

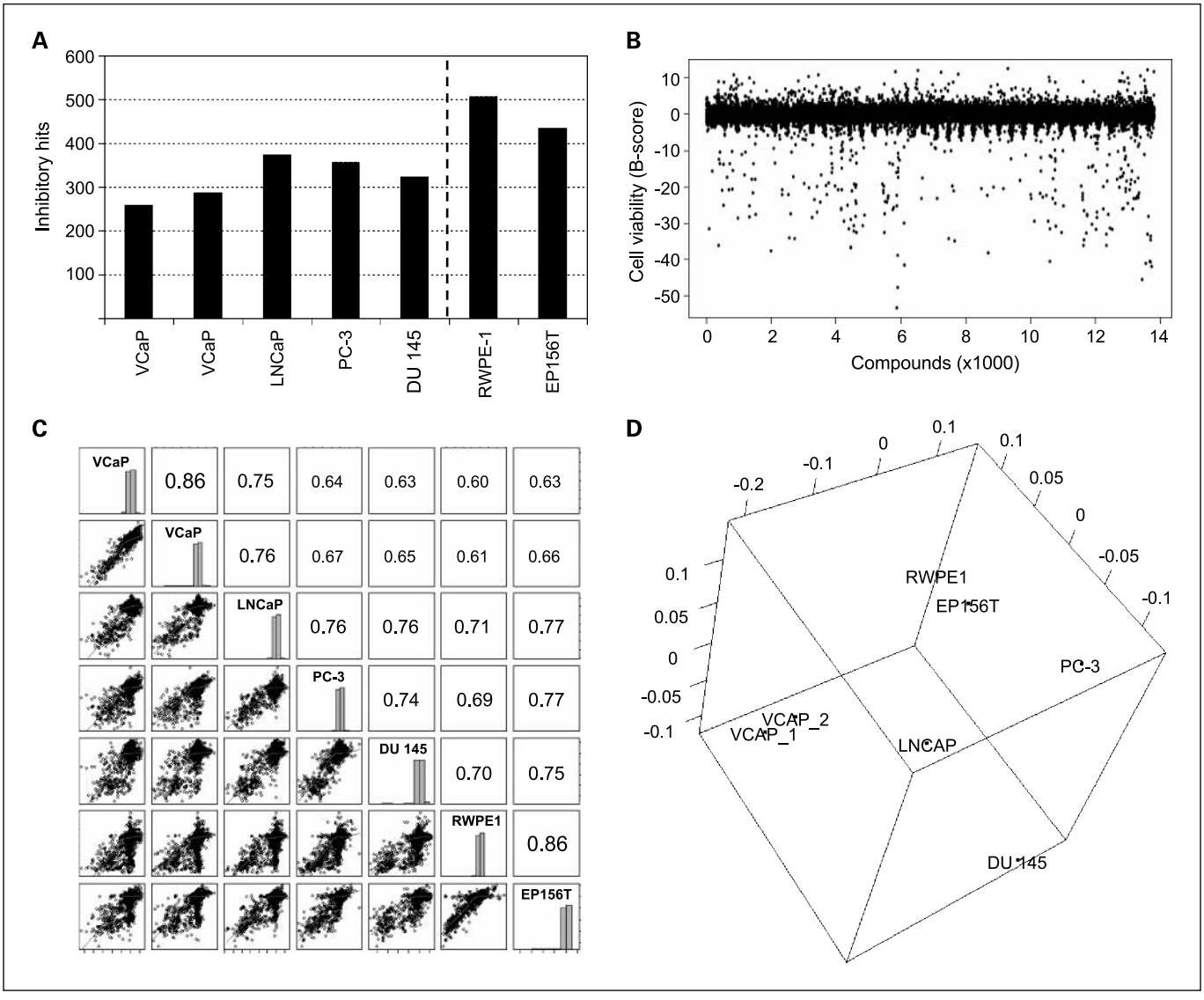

Fig. 1. Cell viability analysis of high-throughput compound screens. *A,* number of hits obtained per HT screen. HTS assay was done twice in TMPRSS2-ERG–positive VCaP cells and once in LNCaP, PC-3, and DU 145 prostate cancer cells as well as in RWPE-1 and EP156T nontumorigenic prostate epithelial cells. *B,* overview of the B-score–normalized data from the high-throughput compound screening in VCaP cells. *C,* pair-wise correlations calculated based on B-score–normalized data. *D,* multidimensional scaling with principal coordinates analysis visualizes the distribution of prostate cell lines based on their compound responses.

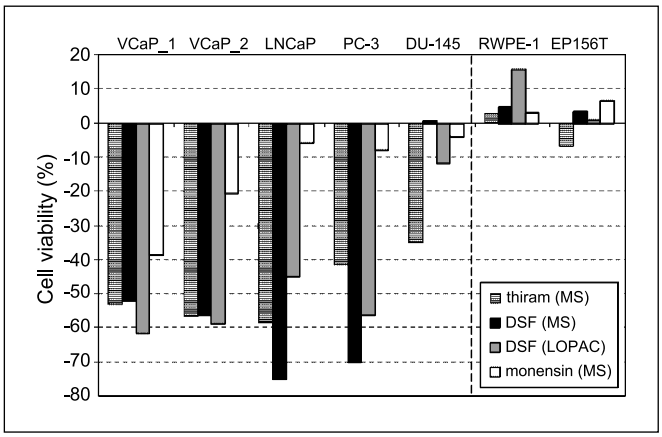

Fig. 2. The absolute cell viability results from the initial HTS for thiram, DSF, and monensin (all at 1 μmol/L concentration) indicate prostate cancer cell selectivity in their growth inhibitory potential. *Right,* compound and the library (*MS,* Microsource Spectrum; LOPAC).

BeadChips (Illumina). The arrays were scanned with the BeadArray Reader (Illumina).

Statistical analysis of gene expression data. The raw gene expression data were quantile normalized and analyzed with the R/Bioconductor software (17). Statistical analysis of differential gene expression after the compound treatments was done using the empirical Bayes statistics implemented in the eBayes function of the limma package (18). Gene expression profiles of the compound-treated samples were compared with the DMSO-treated negative control samples. The threshold for differential expression was $q < 0.05$ after the Benjamini-Hochberg multiple testing correction. The functional Gene Ontology and pathway annotations were analyzed for the sets of differentially expressed genes using DAVID (19, 20). To identify drugs with similar or opposite effects on gene expression, Connectivity Map 02 was used (21).

Xenograft experiments. Athymic nude (Athymic Nude-Foxn 1nu, Harlan Winkelman) male mice, 5 wk of age, were injected s.c. in the flank with 1×10^6 VCaP cells in 200 μL of Matrigel without growth factors (BD Biosciences, Inc.). Tumor volumes were calculated by caliper measurements done weekly to monitor tumor growth (tumor volume = $LW^2 \times 0.56$). When tumor size reached 200 mm^3, the mice were divided into two groups: (*a*) vehicle (olive oil) only and (*b*) DSF (200 mg/kg/d). Mice were treated daily for 3 wk.

Statistical analyses. The hit criteria in HT compound screening (B-score lower than -3 SD from the median) correspond to a *P* value of <0.01. In siRNA screening, hit criteria was mean -2 SD, corresponding to a *P* value of <0.05. Statistical analyses of xenograft growth as well as quantitative reverse transcription PCR results were done by using the Student's *t* test. These results are presented as the mean ± SD. The following *P* values were used to show statistical significance: *, $P < 0.05$; **, $P < 0.01$; and ***, $P < 0.005$.

Results

HTS results. To identify selective antineoplastic compounds, we carried out HTS in AR and TMPRSS2-ERG fusion–positive VCaP cells (two replicate screens), in LNCaP (AR positive, ERG negative), and in PC-3 and DU 145 (both AR and ERG negative), prostate cancer cells as well as in nonmalignant prostate epithelial cells RWPE-1 and EP156T (both AR positive, ERG negative). Because the growth rate of these different cell lines varied, cell amounts were carefully titrated to be on a linear range before HTS. Compound libraries comprising 4,910 small molecule compounds, including most currently marketed drugs, were screened with at least two different concentrations. The cell viability was determined after 3-day incubation with compounds using a fluorescent assay. The compounds that qualified as hits inhibited cell viability (B-score) by at least three SDs from the median of the controls. The number of hits per screen is presented in Fig. 1A. The HTS results showed that the nonmalignant RWPE-1 and EP156T cells were more sensitive to growth inhibition than the prostate cancer cell lines ($P = 0.04$). B-score–normalized data from HT compound screen with VCaP cells is shown in Fig. 1B and, for the other screens, in Supplementary Fig. S1. The pair-wise correlations between the cell viability results (B-scores) obtained from different cell lines were 0.61 to 0.86, reflecting the fact that the majority of compounds had similar effects across all cell lines (Fig. 1C). Multidimensional scaling with principal coordinates analysis was used to visualize the distribution of prostate cell lines based on their compound responses (Fig. 1D), with normal epithelium-derived cell lines forming one group and the different prostate cancer cell lines forming separate clusters.

Because VCaP cells originate from a hormone-refractory prostate cancer patient, are representative of the clinical prostate cancers in terms of the AR and ERG status, and were most distant from nonmalignant prostate epithelial cells in terms of their compound responses, these cells were selected for further exploration. Replicate compound screens in the VCaP cells carried out on different days were highly correlated (r = 0.859) and yielded to a reproducible hit rate of 4.7% with 230 hits (listed in Supplementary Table S1). Several compounds,

Table 1. EC_{50} values (nmol/L) for thiram, DSF and monensin in various prostate epithelial cells

	Thiram	DSF	Monensin
VCaP	95 ± 14	94 ± 19	39 ± 19
DuCaP	72 ± 47	60 ± 18	9 ± 2
LNCaP	222 ± 104	170 ± 36	90 ± 37
LNCaP C4-2	243 ± 224	97 ± 22	42 ± 16
PC-3	>1,000	>1,000	>1,000
DU 145	>10,000	>10,000	>10,000
RWPE-1	>10,000	>10,000	>10,000
EP156T	>10,000	>10,000	>1,000
PrEC	>10,000	>10,000	>1,000

Abbreviation: PrEC, primary prostate epithelial cell.

Downloaded from http://aacrjournals.org/clincancerres/article-pdf/15/19/6070/1983348/6070.pdf by guest on 13 June 2024

such as Taxol, vinblastine sulfate, staurosporine, DSF, mitoxantrone, colcichine, celastrol, and actimomycin D, were identified as hits from multiple libraries included in our HT screen, supporting the overall reliability and functionality of the assay and approach. The HDAC inhibitor TSA was the only selective VCaP inhibitor, which confirms our previous observation where we specifically tested only HDAC inhibitors in prostate cancers (22).

Identification of selective antineoplastic compounds. The B-scores of VCaP, LNCaP, DU 145, and PC-3 prostate cancer cell screens were compared with those seen in the nonmalignant RWPE-1 and EP156T prostate epithelial cells (Supplementary Table S1). In addition to TSA, only three compounds, thiram (tetramethylthiuram disulfide), tetraethylthiuram disulfide (DSF; identified as a hit from two libraries), and monensin sodium, showed selective antineoplastic effects and were therefore selected for further analysis (Supplementary Fig. S2; Fig. 2).

Validation of the HTS results. The EC_{50} values for thiram, DSF, and monensin were determined in VCaP, DuCaP, LNCaP, LNCaP C4-2, DU 145, PC-3, EP156T, RWPE-1 and PrEC cells with a 10-fold dilution series and cell viability measurements. All these compounds inhibit the TMPRSS2-ERG gene fusion–positive VCaP and DuCaP cell viability at nanomolar concentrations (Table 1). LNCaP cells were ~2-fold less sensitive than VCaP cells, and the other prostate cancer cells studied were >10-fold less sensitive. Interestingly, the androgen-independent LNCaP variant C4-2 was as sensitive to DSF and monensin as VCaP cells. The EC_{50} values for thiram and DSF in VCaP cells were >100-fold lower than in nontumorigenic RWPE-1, EP156T, or primary prostate epithelial cell cells (EC_{50} values, >10,000 nmol/L), confirming the selective antineoplastic action of these compounds. Also, monensin was >25-fold more potent in reducing VCaP cell viability than either one of the nonmalignant prostate epithelial cells studied.

Thiram and DSF are structurally homologous members of dithiocarbamate family. In addition to acting as an aldehyde dehydrogenase inhibitor, DSF has been shown to inhibit, e.g., DNA topoisomerases, matrix metalloproteinases, and ABC drug transport proteins, and thereby to have antitumor and chemosensitizing activities (23, 24). Monensin is a Na^+/H^+ antiporter with antibiotic and antimalarial activities. It has been widely used as a biochemical tool to block intracellular protein transport and to improve growth rates in cattle (25). Because DSF is a relatively safe drug used for decades as a Food and Drug Administration–approved alcohol abuse deterrent, it was chosen for more detailed mechanistic studies.

DSF induces the expression of metallothioneins and reduces the expression of ERG and minichromosome maintenance complex genes. To study the growth inhibitory mechanism of DSF in prostate cancer cells, VCaP cells were exposed to 0 (DMSO control) or 1 μmol/L DSF for 3, 6, 24, or 48 hours. Samples were collected and prepared for quantitative PCR and genome-wide gene expression studies. First, ERG and AR mRNA expression was studied in response to DSF by quantitative PCR. The results indicate that ERG mRNA expression is reduced, whereas AR expression in not consistently affected in response to DSF treatment alone (Fig. 3A). Second, for genome-wide expression analysis, early time points were chosen (3, 6, and 24 hours) to gain insights into direct mechanisms rather than secondary alterations caused by DSF. The gene ontology analysis of differentially expressed genes at 3- and 6-hour DSF exposure were enriched in metal-binding activities, whereas the most significantly altered biological process in response to 24-hour exposure was decreased DNA replication (Supplementary Table S2). The metal binding group consisted of zinc transporters and metallothioneins, a group of low molecular weight proteins that regulate the availability of essential metals and protecting cells against DNA damage and oxidative stress. The quantitative PCR results confirmed induction of MT1B, MT1G, MT1F, MT1X, and MT2A mRNA expression in response to 6-hour DSF exposure, whereas at 24-hour metallothionein expression had declined nearly back to the baseline (Fig. 3B). The DNA replication cluster with downregulated mRNA expression was validated by studying minichromosome maintenance complex component (MCM) mRNA expression in response to DSF (Fig. 3C). MCM complexes unwind the double stranded DNA, recruit DNA polymerases, and initiate DNA synthesis. The MCM proteins are highly expressed in malignant human cancer cells and precancerous cells undergoing malignant transformation (26).

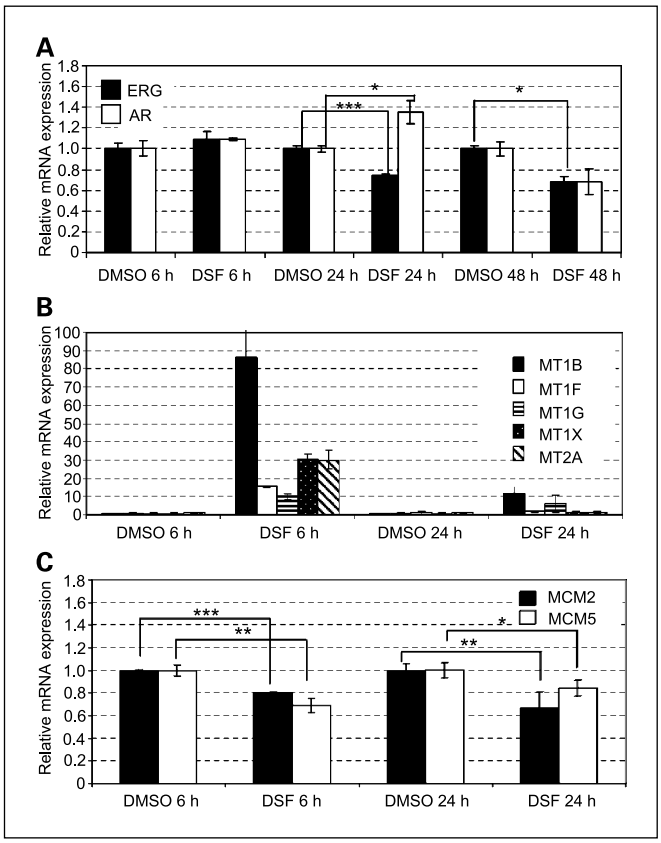

Fig. 3. DSF induced changes in gene expression in VCaP cells. *A,* quantitative reverse transcription-PCR analysis of ERG and AR mRNA expression in VCaP cells in response to 6, 24, and 48 h of exposure to DSF compared with DMSO controls. *B,* quantitative reverse transcription-PCR analysis of metallothionein (MT1B, MT1F, MT1G, MT1X, and MT2A) mRNAs and (*C*) minichromosome MCM (MCM2 and MCM5) mRNAs in VCaP cells exposed to 6 or 24 h DSF compared with DMSO controls.

To get additional clues about the biological processes altered in response to DSF, the differentially expressed genes in DSF exposed VCaP cells after 6 and 24 hours were compared with the >7,000 expression profiles representing drug responses to >1,309 compounds using Connectivity Map.

Downloaded from http://aacrjournals.org/clincancerres/article-pdf/15/19/6070/1983348/6070.pdf by guest on 13 June 2024

The results indicate the highest enrichment with 6-hour DSF treatment and 12,13-EODE (Supplementary Table S3). This compound, 12,13-*cis* epoxide of linoleic acid is generated by neutrophils during the oxidative burst (27). Also irinotecan, a topoisomerase 1 inhibitor was among the most enriched drugs when compared with 6-hour DSF treatment. These correlations support the gene ontology results indicating oxidative stress and inhibition of DNA replication as the DSF-induced biological processes. Interestingly, HDAC inhibitors MS-275 and TSA were among drugs altering gene expression in an opposite direction than DSF (data not shown), indicating that although both HDACi and DSF are potent growth inhibitory compounds in VCaP cells, their mechanisms of action may be completely different.

Metallothioneins and minichromosome maintenance complex genes regulate prostate cancer cell viability. To find out whether metallotioneins and MCM genes affect prostate cancer proliferation, siRNA transfections were done in VCaP and LNCaP prostate cancer cells and cell viability was measured 48 or 72 hours after transfection. The results indicate that silencing of any one of the three genes *MCM5*, *MT1F*, or *MT1G*, is alone sufficient to reduce the proliferation of both VCaP and LNCaP cells (Fig. 4), suggesting that these genes may be among the critical mediators of the molecular mechanisms by which DSF exerts its growth inhibitory effects. For these siRNAs, the silencing of the corresponding gene was confirmed by quantitative PCR in VCaP cells (Supplementary Fig. S3).

DSF inhibits VCaP cell xenograft growth. To study the inhibitory potential of DSF *in vivo* on prostate cancer growth, VCaP cell xenograft experiments were done in immunocompromized mice. Male nude mice were injected s.c. in the flank with VCaP cells. When tumor size was ~200 mm^3, mice were divided into two groups and daily treatments with 200 mg/kg/day DSF in olive oil or olive oil only were administered p.o for 3 weeks. Tumor growth was monitored by measuring tumor size with calipers and calculating the approximate tumor volume. The results indicate that DSF reduced tumor growth up to 40% but was not able to block it, indicating the need for a combinatorial treatment (Fig. 5A).

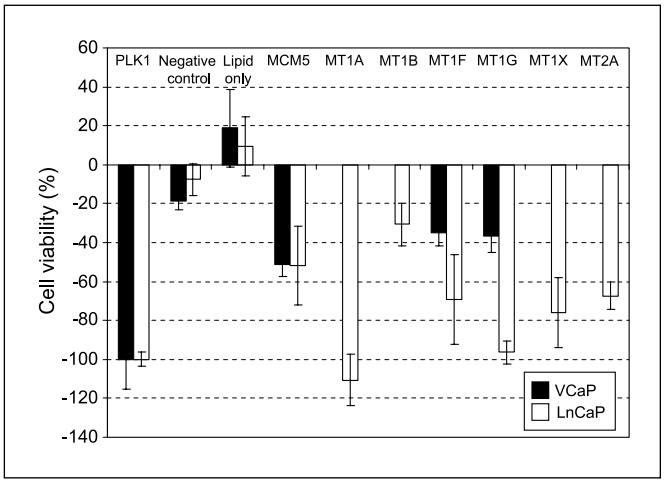

Fig. 4. Metallothioneins and minichromosome MCM regulate prostate cancer cell viability. Cell viability analysis in response to metallothionein (MT1A, MT1B, MT1F, MT1G, MT1X, and MT2A) and minichromosome MCM gene 5 (MCM5) silencing in VCaP and LNCaP prostate cancer cells. Cell viability is presented as percentage of PLK1 siRNA–induced growth inhibition. Only results exceeding the hit limit are shown. AllStars Negative control siRNA and lipid only were used (SiLentFect without siRNAs) as negative controls.

Copper sensitized VCaP cells to DSF-induced cell death. Previous studies with melanoma and breast cancer cells have shown that the growth inhibitory potential of DSF was potentiated with copper or zinc cotreatment (28, 29). Combinatorial effects of DSF and copper or zinc were studied in VCaP cells. VCaP cells were treated with 20 μmol/L $CuCl_2$ alone, DSF alone, or with the DSF-$CuCl_2$ combination and compared with cells treated with DMSO. Similar experiments were done with 20 μmol/L $ZnCl_2$. Apoptotic changes with spherical and detached cells were clearly visible only in the DSF-$CuCl_2$ complex–treated samples after 6-hour treatment. Cell viability assay results indicated a significant reduction in cell viability only in response to DSF-$CuCl_2$ complex treatment (Fig. 5B). $CuCl_2$ and DSF cotreatment reduced AR protein levels and induced poly ADP ribose polymerase cleavage, whereas neither of the agents had an effect alone (Supplementary Fig. S4). Because metallothioneins regulate the intracellular zinc and copper levels and DSF induces metallothionein mRNA expression, we studied metallothionein expression in VCaP cells in response to DSF, $CuCl_2$, and DSF-$CuCl_2$ cotreatment. The results indicate that in response to DSF-$CuCl_2$ cotreatment, the expression of all metallothioneins analyzed is more highly induced, whereas MCM2 and MCM5 expression is even more repressed, than in response to either one of the agents alone (Fig. 5C and D).

Discussion

In this study, we used an unbiased HTS approach to identify clinically compatible drugs to inhibit human prostate cancer growth. Four prostate cancer cell lines and two nontumorigenic prostate epithelial cells were screened with a library of 4,910 drug-like small molecule compounds including most of the currently marketed drugs. We wanted to focus on drugs that are preferentially inhibiting cancer cells. It turned out that the vast majority of anticancer drugs are equally effective in cancer and control cells. For example, docetaxel, currently used in the clinic to treat patients with hormone-refractory prostate cancer, was identified as a nonselective hit in our screen. The other HTS hit compounds already in ongoing clinical trials[5] in prostate cancer included doxorubicin, Taxol/paclitaxel, mitoxantrone, suramin, camptothecin, staurosporine, ixabepilone, 17-AAG, epothilone B, MS-275, and vinblastine sulfate salt. Also, cardiac glycosides, previously identified as hits inhibiting KLK expression in a recent HTS study with breast cancer cells, and reported to have antiproliferative and apoptotic effects also in PC-3, LNCaP, and DU145 cells (30, 31), were identified among antiproliferative compounds in our screen, supporting the overall functionality of our assay. Only a few cancer cell selective growth inhibitory compounds were identified in the HTS experiment. In agreement with our previous data, TSA was among the most selective antiproliferative compounds for VCaP cells (22, 32). The identification of HDAC inhibitors among the selective compounds in an unbiased HTS approach supports our previous conclusions that epigenetic reprogramming is characteristic to ERG-positive prostate cancers. In addition, three novel cancer selective agents, thiram, DSF, and monensin, were

[5] http://www.clinicaltrials.gov

Downloaded from http://aacrjournals.org/clincancerres/article-pdf/15/19/6070/1983348/6070.pdf by guest on 13 June 2024

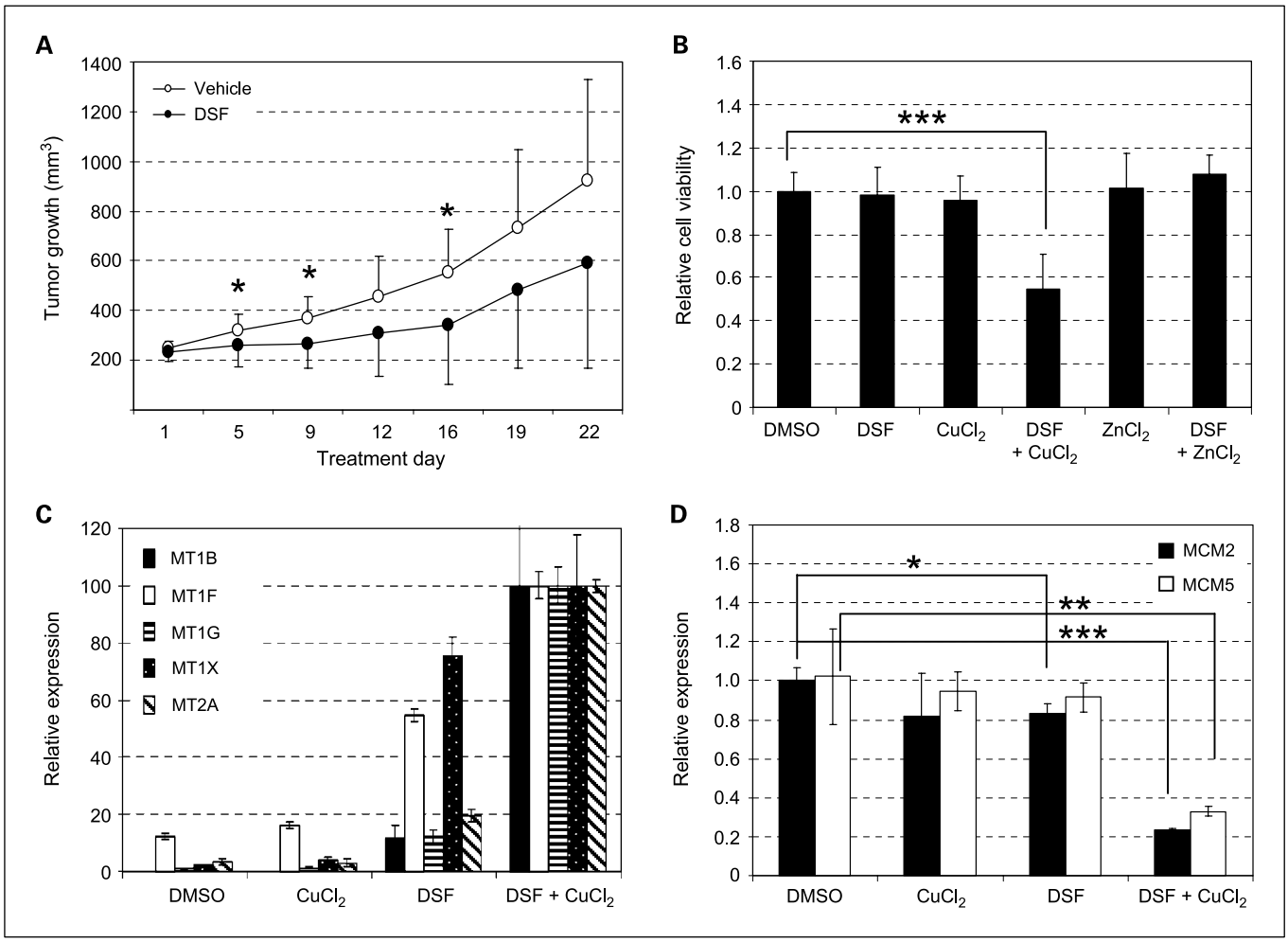

Fig. 5. DSF reduces VCaP xenograft growth and is potentiated by copper in culture. *A,* DSF reduces VCaP cell xenograft growth *in vivo*. Points, mean of tumor volume in each experimental group; bars, SD. Tumor size was significantly decreased in DSF-treated mice when compared with vehicle controls on measurement days 5, 9, and 16. *B,* VCaP cells were exposed to DMSO, DSF, copper or zinc chloride, or a combination of copper or zinc chloride together with DSF for 6 h. Cell viability was measured by a fluorometric cell viability assay and results are presented relative to the DMSO control. *C,* quantitative reverse transcription PCR analysis of metallothionein mRNA expression in VCaP cells in response DMSO, 1 μmol/L DSF, 20 μmol/L $CuCl_2$, or a combination of 20 μmol/L $CuCl_2$ and 1 μmol/L DSF exposure for 6 h. Normalized results are presented relative to $CuCl_2$+DSF exposure. *D,* quantitative reverse transcription PCR analysis of MCM2 and MCM5 expression in same samples as in *C*. Results are presented relative to DMSO control.

identified. These agents inhibit VCaP, LNCaP, and LNCaP C4-2 prostate cancer cell proliferation at nanomolar concentrations, but had little effect on control cells.

Previous studies already indicate that thiram, DSF, and monensin have antitumorigenic effects in culture and in various tumor xenograft models, but their potential in prostate cancer treatment has not been previously explored. Thiram has been shown to block tumor angiogenesis in C6 glioma xenograft model, and to reduce metastases and spontaneous leukemia in rodents (33, 34). However, large doses of thiram have also been reported to cause toxic effects such as neurotoxicity and muscle dysfunction in rats (35). Studies in cultured cells indicate that DSF inhibits myeloma, leukemia, lymphoma, small cell lung cancer, cervical adenocarcinoma, melanoma, neuroblastoma, and colorectal cancer cell survival as well as osteosarcoma invasion (36, 37). Monensin in turn has been reported to inhibit myeloma, renal cell carcinoma, colon cancer, lymphoma, and leukemia cell growth *in vitro* (38-41). Comparison of prostate and breast cancer cell responses to thiram, DSF, or monensin indicated that prostate cancer cells are in general more sensitive to these drugs *in vitro* than breast cancer cells (data not shown).

Due to its excellent safety profile and long-term use as an alcohol deterrent in the clinic, DSF was selected for more detailed mechanistic studies. Genome-wide expression profiling results indicated that DSF induced metallothionein expression and downregulated DNA replication in VCaP cells. Metallothioneins are intracellular proteins that regulate zinc and copper availability, detoxify toxic metals, and protect cells against oxidative stress. Decrease of VCaP cell growth was linked to inhibition of DNA replication by reduced expression of minichromosome maintenance complex genes. *In vivo* studies using VCaP cell xenografts showed reduced tumor growth in response to DSF exposure. However, DSF alone was not able to completely block tumor growth, indicating need for combinatorial approaches.

Previous studies with melanoma and breast cancer cells indicate that DSF given in combination with zinc or copper reduced proliferation *in vitro* at lower concentrations than DSF alone (28, 29). Zinc is known to play an important role in

Downloaded from http://aacrjournals.org/clincancerres/article-pdf/15/19/6070/1983348/6070.pdf by guest on 13 June 2024

various cellular processes such as differentiation by regulating, e.g., transcription factor activities, defense against free radicals, and maintaining genomic stability. In prostate, zinc levels have been reported to be lower in cancer than in normal tissue (42), and increase in dietary zinc has been associated with a decrease in the incidence of prostate cancer (43). A recent study also reported that zinc did not induce DNA damage in normal cells but only in cancer cells (44). However, Zn-DSF cotreatment did not affect VCaP cell viability, whereas copper potentiated the DSF effect and induced cell death. High serum and tissue levels of copper have been found in many types of human cancers including prostate, and hence, copper could act as a tumor-specific sensitizer by, e.g., creating free radicals and thereby DSF response (45). However, physiologic copper levels within VCaP prostate cancer cells are not sufficient to block tumor growth and that additional copper supply could be needed to enhance the DSF response also *in vivo*.

Taken together, our systematic unbiased screen of known drugs and drug-like molecules in prostate models provides the first evidence that prostate cancer cell growth can be efficiently and selectively inhibited by thiram, DSF, and monensin. Thus far, there are clinical trials ongoing only with DSF in non–small cell lung cancer, stage IV melanoma, and metastatic melanoma.[5] Published results of a case report on DSF-treated metastatic melanoma have been very promising (28). Our results indicate that DSF may have potential also in prostate cancer treatment, most likely in combination with other drugs or with specific sensitizers, such as copper. In summary, results from this study provide several novel starting points for preclinical and eventually clinical efforts to treat prostate cancer.

Disclosure of Potential Conflicts of Interest

No potential conflicts of interest were disclosed.

Acknowledgments

We thank Finnish DNA Microarray Centre for performing the Illumina experiments and Niko Sahlberg, Arttu Heinonen, and Jouni Latoniitty for excellent technical assistance with HTS.

Downloaded from http://aacrjournals.org/clincancerres/article-pdf/15/19/6070/1983348/6070.pdf by guest on 13 June 2024

References

1. Tannock IF, de Wit R, Berry WR, et al. Docetaxel plus prednisone or mitoxantrone plus prednisone for advanced prostate cancer. N Engl J Med 2004;351:1502–12.
2. Taichman RS, Loberg RD, Mehra R, Pienta KJ. The evolving biology and treatment of prostate cancer. J Clin Invest 2007;117:2351–61.
3. Tomlins SA, Rhodes DR, Perner S, et al. Recurrent fusion of TMPRSS2 and ETS transcription factor genes in prostate cancer. Science 2005;310:644–8.
4. Nam RK, Sugar L, Yang W, et al. Expression of the TMPRSS2:ERG fusion gene predicts cancer recurrence after surgery for localised prostate cancer. Br J Cancer 2007;97:1690–5.
5. Hermans KG, van Marion R, van Dekken H, Jenster G, van Weerden WM, Trapman J. TMPRSS2:ERG fusion by translocation or interstitial deletion is highly relevant in androgen-dependent prostate cancer, but is bypassed in late-stage androgen receptor-negative prostate cancer. Cancer Res 2006;66:10658–63.
6. Korenchuk S, Lehr JE, MClean L, et al. VCaP, a cell-based model system of human prostate cancer. In Vivo 2001;15:163–8.
7. Tomlins SA, Laxman B, Dhanasekaran SM, et al. Distinct classes of chromosomal rearrangements create oncogenic ETS gene fusions in prostate cancer. Nature 2007;448:595–9.
8. van Bokhoven A, Varella-Garcia M, Korch C, et al. Molecular characterization of human prostate carcinoma cell lines. Prostate 2003;57:205–25.
9. Harris SE, Rong Z, Harris MA, Lubahn DB. Androgen receptor in human prostate carcinoma LNCaP/ADEP cells contains a mutation which alters the specificity of the steroid dependent transcrip-tional activation region. GA: Atlanta; 1990, p. 93.
10. Gaddipati JP, McLeod DG, Heidenberg HB, et al. Frequent detection of codon 877 mutation in the androgen receptor gene in advanced prostate cancers. Cancer Res 1994;54:2861–4.
11. Webber MM, Bello D, Kleinman HK, Hoffman MP. Acinar differentiation by non-malignant immortalized human prostatic epithelial cells and its loss by malignant cells. Carcinogenesis 1997;18:1225–31.
12. Kogan I, Goldfinger N, Milyavsky M, et al. hTERT-immortalized prostate epithelial and stromal-derived cells: an authentic *in vitro* model for differentiation and carcinogenesis. Cancer Res 2006;66:3531–40.
13. Brideau C, Gunter B, Pikounis B, Liaw A. Improved statistical methods for hit selection in high-throughput screening. J Biomol Screen 2003;6:634–47.
14. Gower JC. Some distance properties of latent root and vector methods used in multivariate analysis. Biometrika 1966;53:325–28.
15. Boutros M, Brás LP, Huber W. Analysis of cell-based RNAi screens. Genome Biol 2006;7:R66.
16. Cleveland WS, Grosse E, Shyu MJ. Local regression models. In: Chambers JM, Hastie TJ, editors. Statistical Models in S. New York: Chapman and Hall; 1992, p. 309–76.
17. Gentleman RC, Carey VJ, Bates DM, et al. Bioconductor: open software development for computational biology and bioinformatics. Genome Biol 2004;5:R80.
18. Smyth GK. Linear models and empirical bayes methods for assessing differential expression in microarray experiments. Stat Appl Genet Mol Biol 2004;3:1–25.
19. Dennis G, Jr., Sherman BT, Hosack DA, et al. DAVID: Database for Annotation, Visualization, and Integrated Discovery. Genome Biol 2003;4:3.
20. Huang DW, Sherman BT, Lempicki RA. Systematic and integrative analysis of large gene lists using DAVID Bioinformatics Resources. Nat Protocol 2009;4:44–57.
21. Lamb J. The Connectivity Map: a new tool for biomedical research. Nat Rev Cancer 2007;7:54–60.
22. Björkman M, Iljin K, Halonen P, et al. Defining the molecular action of HDAC inhibitors and synergism with androgen deprivation in ERG-positive prostate cancer. Int J Cancer 2008;123:2774–81.
23. Yakisich JS, Sidén A, Eneroth P, Cruz M. Disulfiram is a potent *in vitro* inhibitor of DNA topoisomerases. Biochem Biophys Res Commun 2001;289:2586–90.
24. Sauna ZE, Shukla S, Ambudkar SV. Disulfiram, an old drug with new potential therapeutic uses for human cancers and fungal infections. Mol Biosystem 2005;1:127–34.
25. Mollenhauer HH, Morré DJ, Rowe LD. Alteration of intracellular traffic by monensin; mechanism, specificity and relationship to toxicity. Biochim Biophys Acta 1990;1031:225–46.
26. Lei M. The MCM complex: its role in DNA replication and implications for cancer therapy. Curr Cancer Drug Targets 2005;5:365–80.
27. Hayakawa M, Sugiyama S, Takamura T, et al. Neutrophils biosynthesize leukotoxin, 9,10-epoxy-12-octadecenoate. Biochem Biophys Res Commun 1986;137:424–30.
28. Brar SS, Grigg C, Wilson KS, et al. Disulfiram inhibits activating transcription factor/cyclic AMP-responsive element binding protein and human melanoma growth in a metal-dependent manner *in vitro*, in mice and in a patient with metastatic disease. Mol Cancer Ther 2004;3:1049–60.
29. Chen D, Cui QC, Yang H, Dou QP. Disulfiram, a clinically used anti-alcoholism drug and copper-binding agent, induces apoptotic cell death in breast cancer cultures and xenografts via inhibition of the proteasome activity. Cancer Res 2006;66:10425–33.
30. McConkey DJ, Lin Y, Nutt LK, Ozel HZ, Newman RA. Cardiac glycosides stimulate Ca2+ increases and apoptosis in androgen-independent, metastatic human prostate adenocarcinoma cells. Cancer Res 2000;60:3807–12.
31. Prassas I, Paliouras M, Datti A, Diamandis EP. High-throughput screening identifies cardiac glycosides as potent inhibitors of human tissue kallikrein expression: implications for cancer therapies. Clin Cancer Res;14:5778–84.
32. Iljin K, Wolf M, Edgren H, et al. TMPRSS2 fusions with oncogenic ETS factors in prostate cancer involve unbalanced genomic rearrangements and are associated with HDAC1 and epigenetic reprogramming. Cancer Res 2006;66:10242–6.
33. Marikovsky M. Thiram inhibits angiogenesis and slows the development of experimental tumours in mice. Br J Cancer 2002;86:779–87.
34. Hasegawa R, Takahashi M, Furukawa F, et al. Carcinogenicity study of tetramethylthiuram disulfide (thiram) in F344 rats. Toxicology 1988;51:155–65.
35. Lee CC, Peters PJ. Neurotoxicity and behavioural effects of thiram in rats. Environ Health Perspectives 1976;17:35–43.
36. Wang W, McLeod HL, Cassidy J. Disulfiram-mediated inhibition of NF-κB activity enhances cytotoxicity of 5-fluorouracil in human colorectal cancer cell lines. Int J Cancer 2003;104:504–11.

37. Wickström M, Danielsson K, Rickardson L, et al. Pharmacological profiling of disulfiram using human tumor cell lines and human tumor cells from patients. Biochem Pharmacol 2007;73:25–33.
38. Park WH, Seol JG, Kim ES, et al. Monensin-mediated growth inhibition in human lymphoma cells through cell cycle arrest and apoptosis. Br J Haematol 2002;119:400–7.
39. Park WH, Kim ES, Jung CW, Kim BK, Lee YY. Monensin-mediated growth inhibition of SNU-C1 colon cancer cells via cell cycle arrest and apoptosis. Int J Oncol 2003;22:377–82.
40. Park WH, Kim ES, Kim BK, Lee YY. Monensin-mediated growth inhibition in NCI-H929 myeloma cells via cell cycle arrest and apoptosis. Int J Oncol 2003;23:197–204.
41. Park WH, Jung CW, Park JO, et al. Monensin inhibits the growth of renal cell carcinoma cells via cell cycle arrest or apoptosis. Int J Oncol 2003;22:855–60.
42. Costello LC, Franklin RB. Novel role of zinc in the regulation of prostate citrate metabolism and its implications in prostate cancer. Prostate 1998;35:285–96.
43. Kristal AR, Stanford JL, Cohen JH, Wicklund K, Patterson RE. Vitamin and mineral supplement use is associated with reduced risk of prostate cancer. Cancer Epidemiol Biomarkers Prev 1999;8:887–92.
44. Sliwinski T, Czechowska A, Kolodziejczak M, Jajte J, Wisniewska-Jarosinska M, Blasiak J. Zinc salts differentially modulate DNA damage in normal and cancer cells. Cell Biol Int 2009;33:542–7.
45. Gupte A, Mumper RJ. Elevated copper and oxidative stress in cancer cells as a target for cancer treatment. Cancer Treat Rev 2009;35:32–46.

Downloaded from http://aacrjournals.org/clincancerres/article-pdf/15/19/6070/1983348/6070.pdf by guest on 13 June 2024